Food & Function

ROYAL SOCIETY OF CHEMISTRY

PAPER

View Article Online
View Journal | View Issue

Open Access Article. Published on 06 March 2025. Downloaded on 3/20/2026 12:09:17 PM.
This article is licensed under a Creative Commons Attribution-NonCommercial 3.0 Unported Licence.

Check for updates

Cite this: *Food Funct.*, 2025, **16**, 2737

Myricetin alleviates high-fat diet-induced atherosclerosis in ApoE$^{-/-}$ mice by regulating bile acid metabolism involved in gut microbiota remodeling†

Yilong Liu,[a] Ruoqi Wang,[a] Jinren Zhou,[b] Qiang Lyu,[c] Xiaoyong Zhao,[a] Xiaochun Yang,[d,e] Kunsong Chen,[a] Zhiwei Gao*[b] and Xian Li *[a,e]

Received 20th January 2025,
Accepted 4th March 2025

DOI: 10.1039/d5fo00374a

rsc.li/food-function

Atherosclerosis poses a significant threat to global health. This study aimed to investigate the effects of myricetin (MYR) on high-fat diet (HFD)-induced atherosclerosis in ApoE$^{-/-}$ mice. Our findings demonstrated that MYR treatment significantly reduced the formation of atherosclerotic plaques, particularly at a high dose of 100 mg kg^{-1} day^{-1}. Additionally, MYR markedly attenuated lipid metabolism disorders in ApoE$^{-/-}$ mice by decreasing body weight, improving serum lipid profiles, and reducing lipid deposition. Analysis of 16S rRNA sequencing revealed that MYR treatment enhanced the abundance of probiotic *g_Lachnospiraceae_NK4A136*, while it reduced that of obesity-associated genera, including *Rikenellaceae_RC9_gut_group* and *Alistipes*. Metabolomic analysis and RT-qPCR tests indicated that MYR upregulated hepatic bile acid biosynthesis, evidenced by increased total bile acid levels and enhanced expression of key enzymes CYP7A1 and CYP8B1, particularly through the classical biosynthetic pathway. Spearman's correlation analysis revealed strong associations between the regulated bile acids and these aforementioned bacteria. Therefore, our results demonstrated that MYR exerts an anti-atherosclerotic effect by modulating the gut-liver axis.

Introduction

Atherosclerosis is a chronic and progressive cardiovascular disease characterized by the hardening and narrowing of arteries due to the gradual buildup of cholesterol plaques.[1] It is a leading cause of global mortality and morbidity, comprising 85% of cardiovascular deaths and 28% of all-cause mortality.[2] The pathologies of atherosclerosis are influenced by a range of risk factors, including hyperglycemia, hyperlipidemia, hypertension, gut dysbiosis, and so on.[3] Current clinical treatments primarily focus on managing these risk factors by utilizing glucose- or lipid-lowering agents. However, prolonged use of these drugs has been associated with a range of adverse effects, such as myopathy, renal damage, and liver function impairment.[4,5] Therefore, it is essential to find effective and safe strategies for the prevention and treatment of atherosclerosis.

Mounting evidence highlights the crucial role of dietary factors in the onset and progression of atherosclerosis.[6,7] Diets high in saturated fats, commonly referred to as high-fat diets (HFD), have been proven to be a major risk factor for the formation of atherosclerotic plaque and the subsequent development of cardiovascular events.[8] HFD can contribute to elevated levels of low-density lipoprotein cholesterol (LDL-C), a known risk factor for atherosclerosis, and may lead to oxidative stress, insulin resistance, and inflammation in the body, accelerating the progression of atherosclerosis.[9,10]

In contrast, increasing evidence suggests that a higher intake of polyphenol-rich foods is associated with a reduced risk of atherosclerosis.[11,12] Myricetin (MYR) is a key member of

[a]*Zhejiang Key Laboratory of Horticultural Crop Quality Improvement, Zhejiang University, Hangzhou 310058, China. E-mail: xianli@zju.edu.cn; Fax: +86-571-88982224; Tel: +86-571-88981263*
[b]*Department of Vascular Surgery, the Second Affiliated Hospital of Zhejiang University School of Medicine, Hangzhou 310009, China. E-mail: 2317157@zju.edu.cn; Tel: +86-18768481862*
[c]*School of Pharmacy, Zhejiang Chinese Medical University, 548, Binwen Road, Hangzhou 310053, China*
[d]*Center for Drug Safety Evaluation and Research, College of Pharmaceutical Sciences, Zhejiang University, Hangzhou, China*
[e]*Shandong (Linyi) Institute of Modern Agriculture, Zhejiang University, Linyi 276000, China*

†Electronic supplementary information (ESI) available: The sequences of the primers for RT-qPCR analysis of gene expression in liver; effects of MYR on the composition of gut microbiota in ApoE$^{-/-}$ mice; identification of the most characteristic gut microbiota in MYR-treated ApoE$^{-/-}$ mice analyzed by LEfSe at different taxonomy levels; correlations between the relative abundance of gut microbiota (top 30 genera) and hepatic bile acids in MYR-treated ApoE$^{-/-}$ mice. See DOI: https://doi.org/10.1039/d5fo00374a

Open Access Article. Published on 06 March 2025. Downloaded on 3/20/2026 12:09:17 PM.
This article is licensed under a Creative Commons Attribution-NonCommercial 3.0 Unported Licence.

the flavonol class of flavonoids, which naturally occurs in various plant-based foods such as berries, citrus, tomatoes, tea, and wine.[13] MYR possesses a unique structure characterized by six hydroxyl groups distributed across its molecular framework and exhibits excellent antioxidant and anti-inflammatory activities.[14,15] It seems to show multiple beneficial effects on cardiovascular health based on its reduction of inflammation and oxidative stress. However, studies on the protective effect of MYR against HFD-induced atherosclerosis and the underlying mechanisms are quite limited.

Recently, significant interest has focused on the intestinal microbiota–host interaction because accumulating evidence has demonstrated that gut microbiota plays a critical role in human health and disease, such as cardiovascular disease.[16,17] There is a complex interplay between microbiota, host metabolism, and the development and progression of atherosclerosis.[18] Bile acids are a class of important mediators in microbiota–host crosstalk, whose metabolism is a key pathway involved in the absorption and excretion of dietary lipids and cholesterol.[19] Bile acids are produced by cholesterol in the liver and further metabolized by gut microbiota, acting as detergents that promote the dissolution, digestion and absorption of fat-soluble vitamins and dietary lipids.[20] Dysregulation of bile acid metabolism will result in an elevated level of serum cholesterol and, consequently, the development of atherosclerosis.[21]

In this study, we investigated the impact of MYR on HFD-induced atherosclerosis in apolipoprotein E-deficient ($ApoE^{-/-}$) mice by analyzing atherosclerotic lesions and hepatic lipid profiles. Further, 16s rRNA sequencing analysis was carried out to study the gut microbiota-related regulation mechanisms of MYR in atherosclerotic mice. Metabolomics analysis of mice liver showed the metabolic differences between healthy and atherosclerosis subjects with or without MYR treatment, and the prominent differential metabolites were significantly enriched in the primary bile acids biosynthesis pathway. Hepatic bile acids contents were then determined by targeted metabolomics analysis, and the expression of genes implicated in hepatic bile acids synthesis was detected. The results provided valuable insights into the mechanisms by which MYR alleviated atherosclerosis, laying a scientific foundation for the development of functional foods enriched with MYR.

Materials and methods

Materials and chemicals

MYR, cholic acid (CA), chenodeoxycholic acid (CDCA), deoxycholic acid (DCA), tauro-cholic acid (TCA), tauro-chenodeoxycholic acid (TCDCA), and tauro-hyodeoxycholic acid (THDCA) standards were brought from Shanghai Yuanye Bio-Technology Co., Ltd (Shanghai, China). Ursodeoxycholic acid (UDCA), hyodeoxycholic acid (HDCA), and tauro-ursodeoxycholic acid (TUDCA) standards were purchased from Aladdin Chemistry Co. Ltd (Shanghai, China). α-Muricholic acid (α-MCA), β-muricholic acid (β-MCA), ω-muricholic acid (ω-MCA), tauro-α-muricholic acid (T-α-MCA), tauro-β-muricholic acid (T-β-MCA), tauro-ω-muricholic acid (T-ω-MCA), and tauro-ursodeoxycholic acid (TDCA) standards were the products of Avanti Polar Lipids, Inc. (Alabaster, AL, USA). Trizol (DR0407100) was purchased from Zhejiang Easydo Biotechnology Ltd (Zhejiang, China). HiScript II 1st Strand cDNA Synthesis Kit and SYBR Green qPCR Master Mix were obtained from Nanjing Vazyme Biotech Co., Ltd (Nanjing, China).

Animal experiments

Twenty-eight male $ApoE^{-/-}$ mice were purchased from Jiangsu GemPharmatech Co., Ltd (Jiangsu, China). They were 8 weeks of age and were housed in a specific-pathogen-free environment under a 12 h light/dark cycle with *ad libitum* access to food and drinking water. After one week of adaptation, mice were randomly divided into four groups (7 mice per group) with different dietary interventions for 14 weeks. The groups included: (1) control group: $ApoE^{-/-}$ mice fed with a standard chow diet; (2) model group: $ApoE^{-/-}$ mice fed with a HFD containing 21% fat and 0.15% cholesterol (Wuxi Fanbo Biotechnology Co., Ltd, Jiangsu, China); (3) low-dose MYR (LMYR) group: HFD-fed $ApoE^{-/-}$ mice treated with a low dose of MYR at 50 mg kg^{-1} animal body weight (BW); (4) high-dose MYR (HMYR) group: HFD-fed $ApoE^{-/-}$ mice treated with a high dose of MYR (100 mg per kg BW). Low- or high-dose MYR was administered to the mice by gavage once daily, with the Control and Model group mice receiving an equivalent volume of distilled water. The doses of MYR were chosen based on a preliminary experiment. Body weight measurement started from the first week of the study and continued weekly throughout the entire experiment for each mouse. Fecal samples were collected at the final three days of the experiment and stored at −80 °C for subsequent analysis.

After 14 weeks, the mice were fasted overnight, weighed, and then underwent blood collection from the orbital vein, followed by euthanasia through decapitation. The heart along with aorta was separated carefully and perfused with phosphate buffered saline (PBS). Tissues including liver, epididymal white adipose tissue (Epi-WAT), and perirenal white adipose tissue (Per-WAT) were collected, weighed and then stored at −80 °C until analysis. All animal experiment protocols were conducted according to the Pharmacology Research & Perspectives policy supplied by the Committee of Animal Research at Zhejiang Chinese Medical University (IACUC-20250113-12).

Serum biochemical indicators analysis

After blood collection, serum was separated by centrifugation at 3000 *g* for 15 min at 4 °C. Total cholesterol (TC), triglyceride (TG), high-density lipoprotein-cholesterol (HDL-C), low-density lipoprotein-cholesterol (LDL-C), and glucose levels in serum were analyzed by kits (Ningbo Purebio Biotechnology Co., Ltd, Ningbo, China) according to the manufacturer's protocol.

 This journal is © The Royal Society of Chemistry 2025

Open Access Article. Published on 06 March 2025. Downloaded on 3/20/2026 12:09:17 PM.
This article is licensed under a Creative Commons Attribution-NonCommercial 3.0 Unported Licence.

Evaluation of atherosclerosis and histological analysis

The entire aorta from aortic root to the iliac artery branch was cleaned by PBS and fixed with 4% paraformaldehyde solution. Then, the aorta was opened longitudinally and stained with Oil Red O to visualize atherosclerotic plaques. The percentage of the aorta occupied by plaque was assessed as an indicator of the severity of atherosclerosis and quantified using Image J software. The heart along with aorta was fixed with 4% paraformaldehyde and embedded in an optimal cutting temperature medium. Frozen 10 μm-thick sections were cut and the sequential cross-sections of the aortic root were stained using Oil Red O.

Liver tissue samples were fixed with 4% paraformaldehyde solution, embedded in paraffin, and then stained with Haematoxylin-eosin (H&E) or Oil Red O. The stained section was visualized under a microscope (Olympus DP20, Japan) through the DP2-BSW image analysis software system with a magnification of 200×.

Nontargeted hepatic metabolomics analysis

A total of 100 mg liver sample was added to 1 mL ice-methanol with internal standard and vortexed for 15 s. The sample was then subjected to ultrasonic extraction for 30 min using an ultrasonic cleaning machine (JBT/C-YCL500T/3P, Jining SINOBEST Machineries Co., Ltd, Shandong, China) at an ultrasonic power of 30 W and a frequency of 60 kHz. After centrifugation at 12 000 rpm for 10 min at 4 °C, the supernatant was collected for the following analysis.

Liquid chromatography-tandem mass spectrometry (LC-MS/MS) analysis was performed as described in a previous study with minor modifications.[22] An ultrahigh-performance liquid chromatography (UPLC) system (Acquity I-class, Waters, 116 Milford, USA) was coupled with a Waters Xevo G2-XS QTOF mass spectrometer (Waters, 117 Manchester, UK). Separation was achieved using a Waters HSS T3 column (1.8 μm, 100 mm × 2.1 mm, Waters 118 Corporation, Milford, MA, USA). The column temperature was set at 40 °C. The samples temperature was maintained at 4 °C with an injection volume of 2 μL and a flow rate of 0.3 mL min^{-1}. The mobile phase was 0.1% formic acid in water (A) and 0.1% formic acid in acetonitrile (B). The gradient was as follows: 0–2 min, 20% B; 2–12 min, 20%-52% B; 12–18 min, 52%–65% B; 18–22 min, 65%–90% B; 22–26 min, 90%–20% B; 26–30 min, 20% B.

The raw data was pre-processed in MZmine 2 software for peak picking and alignment. Potential biomarkers were identified by matching mass-to-charge ratio (m/z) and MS/MS fragment ions from the online databases including the Human Metabolome Database (**https://www.Hmdb.ca**) and MassBank (**https://massbank.jp**). The partial least squares discriminant analysis (PLS-DA) and metabolic pathway enrichment analysis were performed by using MetaboAnalyst 5.0 (**https://www.Metaboanalyst.ca**).

Targeted bile acids analysis

Targeted analysis of bile acids was conducted by UPLC-Q-TOF/MS. The peak annotation and quantitation were analyzed on Waters MassLynx software (version 4.2, Waters Corp, Milford, MA, USA).

Microbiota analysis

The abundance and structure of gut microbiota were determined by 16S rRNA analysis. Bacterial DNA was extracted from fecal samples using the E.Z.N.A. soil DNA Kit (Omega Bio-tek Norcross, GA, USA) and the quality was determined by 1.0% agarose gel electrophoresis. The bacterial 16S rRNA gene V3–V4 region was amplified using forward primer (5′-ACTCCTACGGGAGGCAGCAG-3′) and the reverse primer (5′-GGACTACHVGGGTWTCTAAT-3′). The purified amplicons were subjected to paired-end sequencing on an Illumina MiSeq PE300 platform (Illumina, San Diego, USA) according to the standard protocols by Majorbio Bio-Pharm Technology Co. Ltd (Shanghai, China). Raw files were filtered using QIIME, and the sequences were matched against a high-quality 16S rRNA sequence from the Green Genes database after removing the chimeras. Operational taxonomic units were generated by 97% similarity cutoff using UPARSE and classified based on the 16S rRNA gene Silva database.

Expression of key genes related to hepatic bile acids synthesis

Total RNA was extracted using Trizol reagent (Easydo, Zhejiang, China). cDNA was synthesized with HiScript II 1st Strand cDNA Synthesis Kit (+gDNA wiper; Vazyme). qRT-PCR test was performed on a Bio-Rad CFX96 instrument (Bio-Rad) and GAPDH was used as the internal reference gene. Expression of genes was calculated by the $2^{-\Delta\Delta Ct}$ method. The primers used in the present study were shown in Table S1.†

Statistical analysis

Statistical analysis was performed by using Student's t-test, with $p < 0.05$ as statistically significant. α-Diversity index was calculated with Mothur 1.30.2, and beta diversity was estimated with QIIME 1.9.1. Principal coordinate analysis (PCoA) was performed based on the Bray–Curtis on OUT level. All graphs were conducted by GraphPad Prism 9.0 (GraphPad Software, San Diego, CA, USA). Data were expressed as mean ± standard error of the mean (SEM) which were indicated by error bars.

Results and discussion

MYR attenuated HFD-induced atherosclerosis in ApoE$^{-/-}$ mice

ApoE is a crucial protein engaged in lipid transport and metabolism. The ApoE$^{-/-}$ mice are genetically engineered to lack the *ApoE* gene and display impaired clearance of large atherogenic particles from the circulation. Atherogenesis would be notably accelerated in HFD-fed ApoE$^{-/-}$ mice, and consequently develop aortic lesions.[23] Herein, in order to investigate the anti-atherosclerotic effects of MYR, ApoE$^{-/-}$ mice were fed with HFD and orally administrated with MYR at the dosage of 50 or 100 mg per kg BW. After 14 weeks of HFD feeding with or without MYR treatment, the key initiating

Open Access Article. Published on 06 March 2025. Downloaded on 3/20/2026 12:09:17 PM.
This article is licensed under a Creative Commons Attribution-NonCommercial 3.0 Unported Licence.

events in atherosclerosis were assessed (Fig. 1). HFD induced a significant elevation in body weight in the Model group relative to the Control, while the body weight gain was significantly attenuated in the HMYR treatment group (Fig. 1A). At the end of the animal experiment (14-weeks), the body weight of HFD mice was 37.77 ± 0.88 g, which was significantly higher

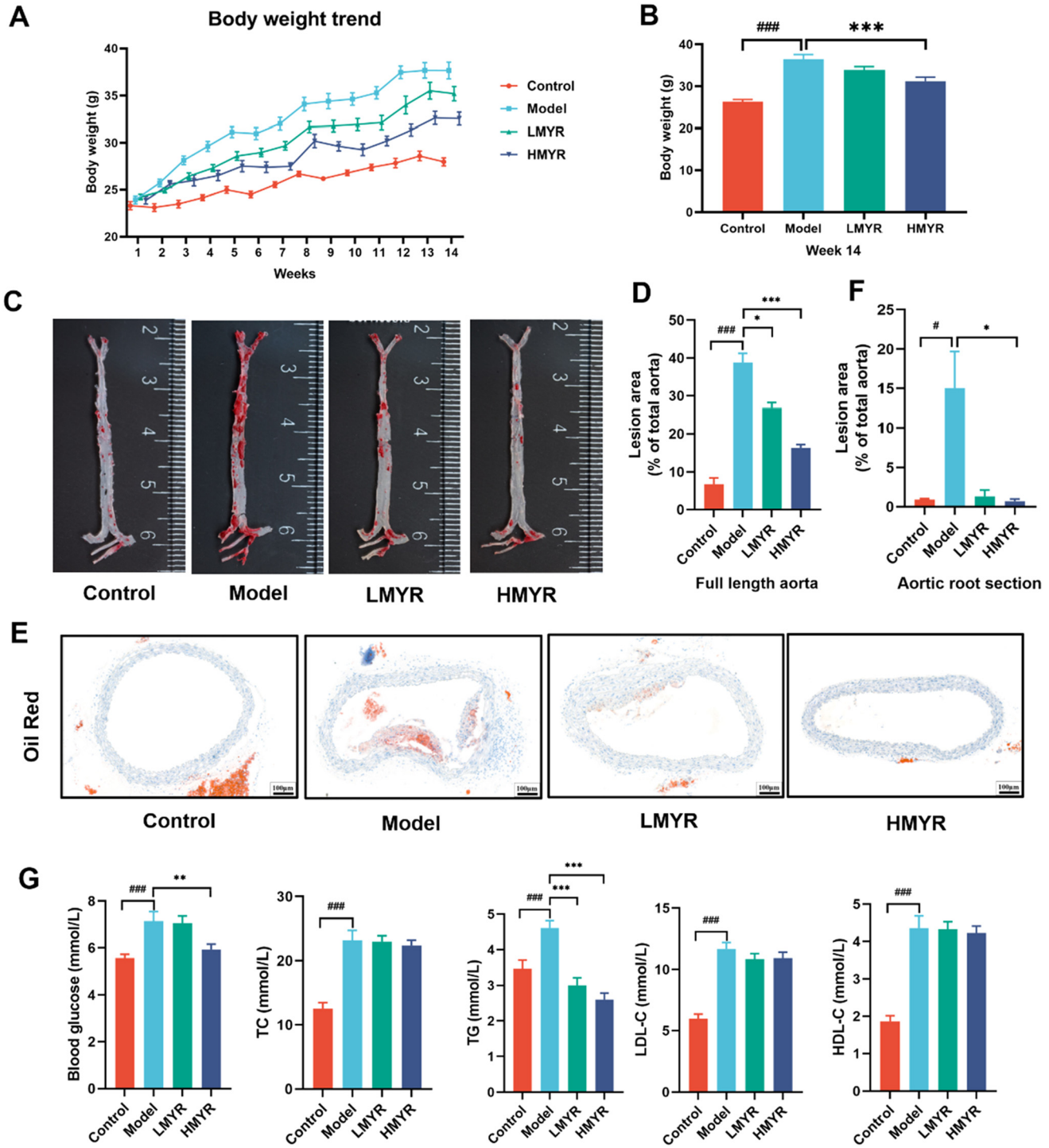

Fig. 1 Effects of myricetin (MYR) on development of atherosclerotic lesions in ApoE$^{-/-}$ mice. (A) Average body weight per group through the entire 14-week period. (B) Mice body weight of week 14. (C) Representative images of oil red O staining of aorta. (D) Quantitative analysis of plaque area in the entire aorta. (E) Representative image of oil red O staining in aortic root sections. (F) Quantitative analysis of the lesion areas in the aortic root. (G) Serum levels of blood glucose, total cholesterol (TC), triglyceride (TG), low-density lipoprotein cholesterol (LDL-C), and high-density lipoprotein cholesterol (HDL-C). Data were expressed as the mean ± SEM (n = 7 per group). # $p < 0.05$, ### $p < 0.001$, Control *vs.* Model; * $p < 0.05$, ** $p < 0.01$, *** $p < 0.001$, LMYR, HMYR *vs.* Model. Control (normal diet fed), Model (high-fat diet fed), LMYR (HFD + Myricetin 50 mg per kg BW), HMYR (HFD + Myricetin 100 mg per kg BW).

 This journal is © The Royal Society of Chemistry 2025

Open Access Article. Published on 06 March 2025. Downloaded on 3/20/2026 12:09:17 PM.
This article is licensed under a Creative Commons Attribution-NonCommercial 3.0 Unported Licence.

than that of the Control group mice (28.21 ± 0.42 g) at the same stage ($p < 0.001$) (Fig. 1B). Treatments of the HFD mice with HMYR resulted in significantly decreased body weight ($p < 0.001$), reduced by 13.66% (32.61 ± 0.70 g) at week 14 (Fig. 1B). The Model group showed markedly larger atherosclerotic lesion areas than the Control group after 14 weeks of HFD feeding, demonstrating the successful establishment of the atherosclerosis model. However, MYR administration significantly decreased the plaque areas in a dose-dependent manner (Fig. 1C and D). Compared to the Model group, the lesion areas were reduced by 30.87% and 57.96% in the LMYR and HMYR groups, respectively (Fig. 1D). Similarly, the lesion areas in the aortic root were also reduced by MYR treatment (Fig. 1E and F). Quercetin and kaempferol, another two common flavonols differing from MYR only in B-ring hydroxylation, were reported to reduce atherosclerosis lesion area in ApoE$^{-/-}$ mice by 2.44% to 28.50% at different doses.[24] It appears that the efficacy of MYR in reducing plaque formation surpasses that of quercetin or kaempferol.

Blood glucose levels and the concentrations of serum TC, TG, LDL-C, and HDL-C are important indicators for evaluating the risk of atherosclerosis.[25] In our study, these indicators were significantly elevated in the Model group compared to the Control group. However, treatment with HMYR lead to a remarkable reduction in blood glucose levels ($p < 0.01$) and serum TG levels ($p < 0.001$) (Fig. 1G). Elevated TG levels, particularly in the form of remnant lipoproteins, are a known risk factor for the development of atherosclerosis. These lipoproteins can promote the accumulation of cholesterol in the arterial wall and trigger inflammatory responses that contribute to plaque formation.[26,27] In the ApoE knockout mouse model, which lacks functional ApoE and exhibits hyperlipidemia with a predominant increase in remnant lipoproteins,[28] the reduction in serum TG likely reflects a decrease in the production or secretion of these atherogenic particles.

Our findings suggested that MYR modulated lipid metabolism and reduced atherosclerotic risk by lowering serum TG levels. This effect aligns with previous studies demonstrating that MYR could ameliorate insulin resistance and improve lipid profiles in various animal models of dyslipidemia, such as streptozotocin-induced diabetic mice[29,30] and fructose-fed rats.[31] In these models, MYR treatment resulted in significant reductions in blood glucose levels and improvements in lipid metabolism, indicating its potential therapeutic role in both metabolic and cardiovascular diseases.

Additionally, compared with the Control, HFD feeding led to a significant increase in the weight of the liver, Epi-WAT, and Per-WAT in the Model, while such weight gains were significantly reduced by HMYR treatment (Fig. 2A). H&E staining or Oil Red O staining results showed HFD-induced fatty infiltration in liver tissue and an obvious accumulation of lipid droplets in hepatocytes in the ApoE$^{-/-}$ mice. However, MYR treatment evidently alleviated these pathological changes and the hepatic lobule structure was arranged by orderliness and tightness (Fig. 2B). These results confirmed other reported lipid-lowering effect of MYR, which could decrease hepatic lipid synthesis and attenuate HFD-induced nonalcoholic fatty liver disease.[32] Altogether, the above findings suggested that HFD accelerated the progression of atherosclerosis, while MYR intervention could effectively inhibit the atherosclerotic plaques accumulation, improve serum profiles, and decrease hepatic lipid accumulation in atherosclerotic mice, particularly at the high dose. Following the anti-atherosclerotic mechanism of MYR was analyzed among the Control, Model, and HMYR groups.

MYR remodeled gut microbiota in ApoE$^{-/-}$ mice

The gut microbiota plays an important role in the cholesterol and lipid metabolism, affecting the development of atherosclerotic plaques.[18] Herein, the structural alteration of the gut microbiota in response to MYR treatment was analyzed. The Ace and Sobs indices are frequently used to evaluate microbial community diversity. The Ace index provides an estimate of the total species richness by factoring in both observed species and rare species. It is particularly useful for accounting for underrepresented rare species. In contrast, the Sobs index directly counts the number of species observed in the sample, offering a straightforward measure of species richness without adjustments for rare species. Together, these indices give complementary perspectives on the diversity and richness of the community. Compared to the Control, the α-diversity index including Ace and Sobs index was significantly decreased in Model group and the effect was reversed by HMYR treatment (Fig. 3A). Similar trends were observed in the Shannon and Chao indexes (Fig. S1A†). Results indicated that treatment with MYR improved the diversity and richness of the microbial community, and such improvement was consistent with the effect observed in rats with HFD-induced nonalcoholic fatty liver disease following MYR supplementation.[32] Principal component analysis and PCoA illustrated that gut microbiota components were distinctly separated among these three groups, which suggested MYR remarkably changed the microbial community structure (Fig. 3B).

The relative abundances of bacteria at various taxonomic levels were determined to investigate the microbial composition alteration induced by MYR treatment. The top 15 bacteria at phylum and family levels were presented in Fig. S1B† and Fig. 3C, respectively. Compared with the Control, the relative abundance of *f*_Lactobacillaceae was significantly decreased, and that of *f*_Rikenellaceae and *f*_Marinifilaceae were increased in the Model group (Fig. 4A). However, HMYR treatment significantly reversed the trend and decreased the relative abundance of *f*_Lachnospiraceae (Fig. 4A).

At the genus level, heatmap analysis revealed significant shifts in microbial populations across the three experimental groups (Fig. S1C†). HMYR treatment significantly reversed the decreased abundance of *g_Lactobacillus* and *g_Lachnospiraceae_NK4A136* in HFD-induced ApoE$^{-/-}$ mice (Fig. 4B). By contrast, the abundance of *g_Alistipes*, *g_Rikenellaceae_RC9_gut_group*, *g_Blautia*, *g_Rikenella*, *g_Odoribacter*, and *g_Lachnoclostridium* markedly increased in HFD group (Fig. 4B), and these trends were in accordance with a previous discovery,[21] and were reversed by HMYR treatment (Fig. 4B).

Open Access Article. Published on 06 March 2025. Downloaded on 3/20/2026 12:09:17 PM.
This article is licensed under a Creative Commons Attribution-NonCommercial 3.0 Unported Licence.

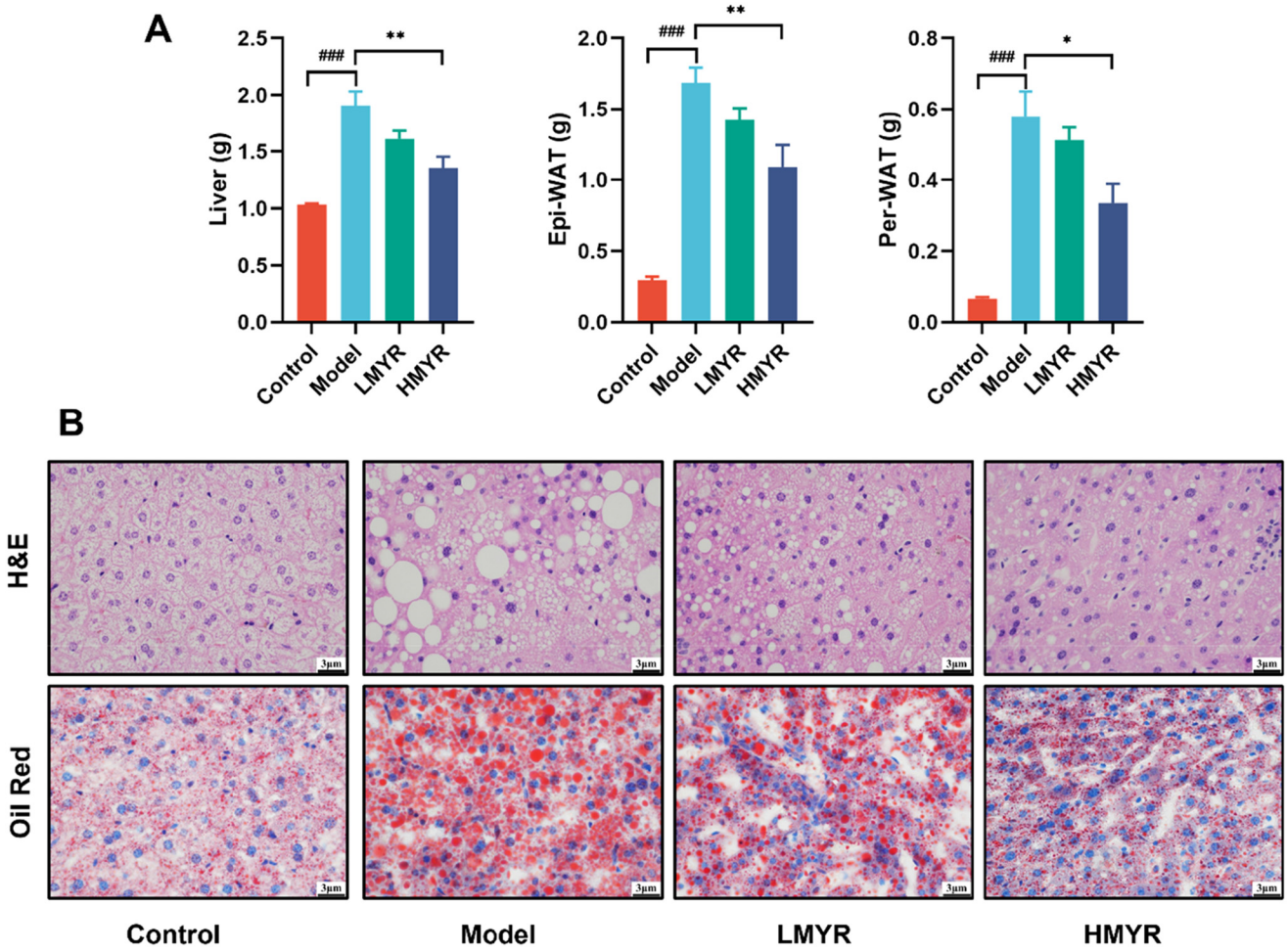

Fig. 2 Effects of MYR on liver and adipose tissue in ApoE$^{-/-}$ mice. (A) Weight of liver, epididymal white adipose tissue (Epi-WAT), and perirenal WAT (Per-WAT). (B) The representative images of Hematoxylin & eosin staining (H&E) and oil red O staining in liver. Data were expressed as the mean ± SEM (n = 7 per group). ### $p < 0.001$, Control *vs.* Model; * $p < 0.05$, ** $p < 0.01$, LMYR, HMYR *vs.* Model.

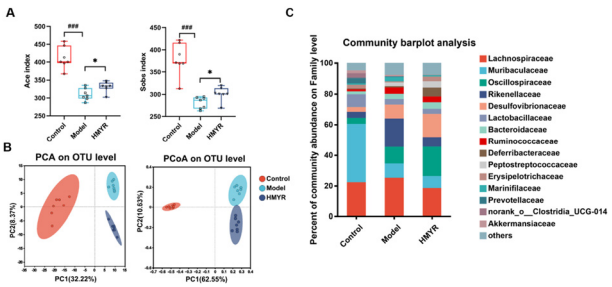

Fig. 3 Effects of MYR on the composition of gut microbiota in ApoE$^{-/-}$ mice. (A) α-Diversity of the gut microbiota measured by Ace, Sobs index. (B) Principal component analysis (PCA) and principal coordinate analysis (PCoA) based on the Bray–Curtis. (C) Microbial community composition at the family level. Data were expressed as the mean ± SEM (n = 7 per group). ### $p < 0.001$, Control *vs.* Model; * $p < 0.05$, HMYR *vs.* Model.

Linear discriminant analysis Effect Size (LEfSe) analysis with a linear discriminant analysis (LDA) score ≥3.5 revealed different sets of bacterial enrichment among three groups (Fig. S2†). In particular, the typically enriched bacterial genus in both Control and HMYR group was *g_Lachnospiraceae_NK4A136*, whereas *g_Blautia*, *g_Rikenellaceae_RC9_gut_group*, and *g_Alistipes* were enriched in the Model group (Fig. S2A–C†). Reports showed that these differentially abundant microbes was linked to several metabolic and inflammatory disorders. For instance, *Lachnospiraceae_NK4A136* group has been reported to be negatively correlated with TG levels and obesity in previous studies.[33,34] In our study, the abundance of *Lachnospiraceae_NK4A136* was also found to be negatively related to the progression of atherosclerosis in HFD-fed ApoE$^{-/-}$ mice, and the trend was significantly reversed by MYR administration (Fig. 4B). Hence, our study confirmed that the abundance of *Lachnospiraceae_NK4A136* group was inversely related to the progression of atherosclerosis, further supporting its role in modulating lipid metabolism and cardiovascular health. The abundance of *g_Alistipes* was reported to be significantly increased in both HFD-induced obese mice and obese population,[35,36] and *g_Blautia* was found to be associated with

This journal is © The Royal Society of Chemistry 2025

Open Access Article. Published on 06 March 2025. Downloaded on 3/20/2026 12:09:17 PM.
This article is licensed under a Creative Commons Attribution-NonCommercial 3.0 Unported Licence.

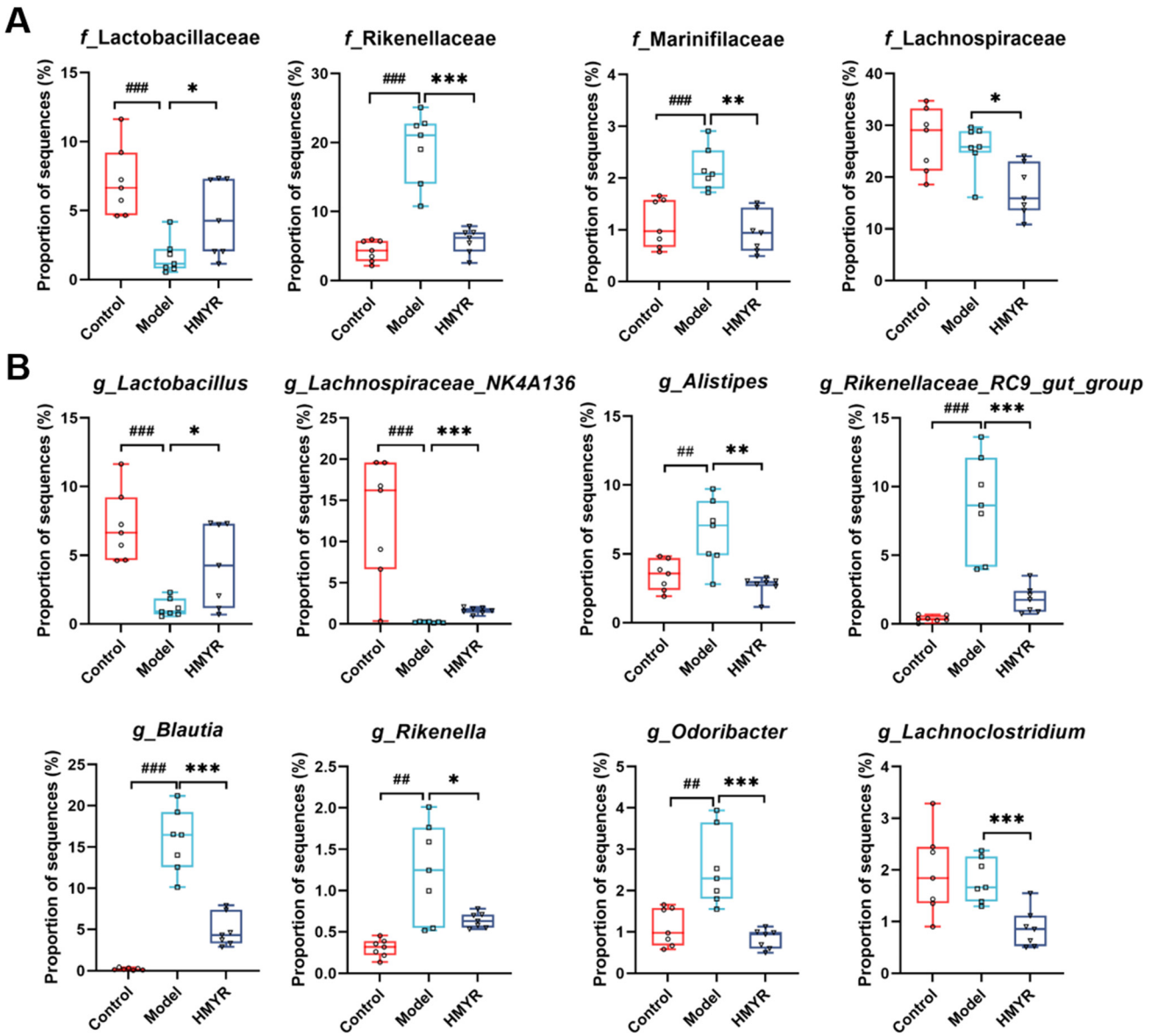

Fig. 4 Relative abundance of gut microbiota at different levels among the three groups in ApoE$^{-/-}$ mice. (A) Relative abundance of major differential gut microbiota at the family level. (B) Relative abundance of major differential gut microbiota at the genus level. Data are expressed as the mean ± SEM (n = 7 per group). ## $p < 0.01$, ### $p < 0.001$, Control *vs.* Model; * $p < 0.05$, ** $p < 0.01$, *** $p < 0.001$, HMYR *vs.* Model.

visceral fat accumulation in adults of age ranging from 20 to 76.[37] However, HMYR treatment significantly decreased the abundance of *g_Alistipes* and *g_Blautia*. These results suggested that MYR might exert anti-atherosclerotic effect through modulating the obese-associated gut microbiota in ApoE$^{-/-}$ mice.

Several factors could influence microbiota changes such as diet, host genetics, and microbial interactions. HFD is a potent driver of microbial dysbiosis, promoting the expansion of pro-inflammatory and pathogenic bacteria while reducing beneficial commensals.[38] MYR, as a bioactive compound, appears to modulate these changes by restoring the balance of gut microbiota. Its antioxidant and anti-inflammatory properties may contribute to gut health and potentially slow atherosclerosis progression.[13,14]

MYR regulated hepatic metabolomic phenotypes in ApoE$^{-/-}$ mice

Hepatic cholesterol metabolism dysfunction was closely associated with cholesterol accumulation in the arterial intima and drove the development of atherosclerosis.[39,40] To investigate the effect of MYR treatment on hepatic metabolism, untargeted metabolomic analysis was conducted in liver, the primary organ responsible for cholesterol metabolism.[41,42] As shown in Fig. 5A, PLS-DA results indicated the apparent distinct clustering of metabolites among the Control, Model, and HMYR groups. There were 119 metabolites identified and

Open Access Article. Published on 06 March 2025. Downloaded on 3/20/2026 12:09:17 PM.
This article is licensed under a Creative Commons Attribution-NonCommercial 3.0 Unported Licence.

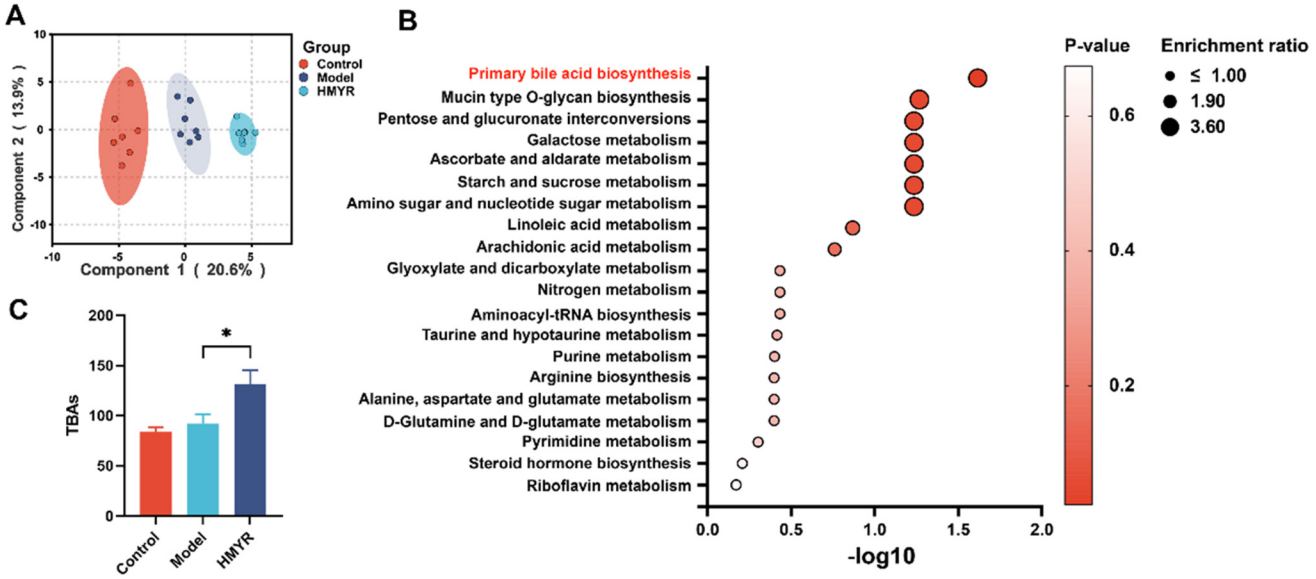

Fig. 5 Effects of MYR on the metabolic profile in ApoE$^{-/-}$ mice. (A) PLS-DA score plot of the hepatic untargeted metabolome. (B) Enrichment analysis of the prominent metabolites in MYR-treated ApoE$^{-/-}$ mice. (C) Hepatic total bile acids (TBAs) in MYR-treated ApoE$^{-/-}$ mice. Data were expressed as the mean ± SEM (n = 7 per group). * $p < 0.05$, HMYR *vs.* Model.

annotated in the liver of all groups. The KEGG pathway enrichment analysis showed the effect of HMYR on these metabolites and revealed that the most significant pathway was primary bile acids biosynthesis (Fig. 5B). Total bile acids in liver were significantly increased in the HMYR group, compared to Model (Fig. 5C). Previous researches have shown that elevation of bile acids synthesis could alleviate lipid accumulation and improve insulin sensitivity in obese mice.[43,44]

Targeted and quantitative analysis was performed to further investigate the effect of MYR on bile acids (Fig. 6A). The results indicated that CA, ω-MCA, and corresponding tauro-conjugated bile acids including TCA and T-ω-MCA were significantly increased after HMYR treatment. However, CDCA, β-MCA, TCDCA, and THDCA were decreased in HMYR group, compared to the Model.

The bile acids were produced in the liver, secreted into duodenum, reabsorbed in the ileum, and transported back to the liver to be recycled. In the gut, bile acids were deconjugated and converted by the microbiota, while the composition of microbiota was also altered by the anti-microbial effect of bile acids.[45] Spearman correlation analysis was performed to explore the associations between gut microbiota and bile acids in HMYR-treated ApoE$^{-/-}$ mice (Fig. S3†). Results showed that CDCA and THDCA were positively correlated with *g_Rikenellaceae_RC9_gut_group* and *g_Alistipes*, and negatively correlated with *g_Lachnospiraceae_NK4A136*. These results suggested that the effect of MYR on atherosclerosis may be associated with the regulation of gut-liver axis.

MYR regulated key genes of hepatic bile acids synthesis pathway in ApoE$^{-/-}$ mice

Based on the hepatic targeted bile acids profiles, the major primary bile acids including CA and CDCA significantly increased after MYR treatment. Therefore, the effect of MYR on hepatic key genes in regulation of bile acids synthesis was investigated (Fig. 6B). Bile acids biosynthesis from cholesterol was initiated by cholesterol 7α-hydroxylase (*CYP7A1*) in the classic pathway or sterol 27-hydroxylase (*CYP27A1*) in the alternative pathway in the liver.[20] Particularly, *CYP7A1* encodes the rate-limiting enzyme for bile acids biosynthesis.[46] Our results showed that the hepatic expression of *CYP7A1* and sterol 12α-hydroxylase (*CYP8B1*) in bile acids synthesis classic pathway were significantly increased in the HMYR group compared to the Model (Fig. 6B). Similarly, MYR was reported to be able to promote the lipid metabolism and excretion *via* up-regulating *CYP7A1* in hyperlipidemia mice.[47] In bile acids alternative classic pathway, the expression of *CYP27A1* was increased after HMYR treatment, however, the key gene expression of steroid 7α-hydroxylase (*CYP7B1*) was significantly decreased (Fig. 6B). As well, the HMYR group showed an increased production of CA and a decreased level of CDCA, indicating that MYR up-regulated hepatic bile acids synthesis in HFD-fed ApoE$^{-/-}$ mice mainly through the classical pathway.

MYR regulated gut-liver axis in ApoE$^{-/-}$ mice

Bile acids synthesis and excretion constitute a primary pathway in cholesterol and lipid catabolism, implicating their involvement in diverse metabolic disorders.[48] Previous studies have shown that bile acids act as antimicrobial agents and signaling molecules, selectively shaping the gut microbiota composition.[49] In turn, gut microbiota influence bile acid metabolism and affect host lipid metabolism and inflammation.[50] Our results indicated that the impact of MYR on atherosclerosis was associated with the regulation of bile acids synthesis

Open Access Article. Published on 06 March 2025. Downloaded on 3/20/2026 12:09:17 PM.
This article is licensed under a Creative Commons Attribution-NonCommercial 3.0 Unported Licence.

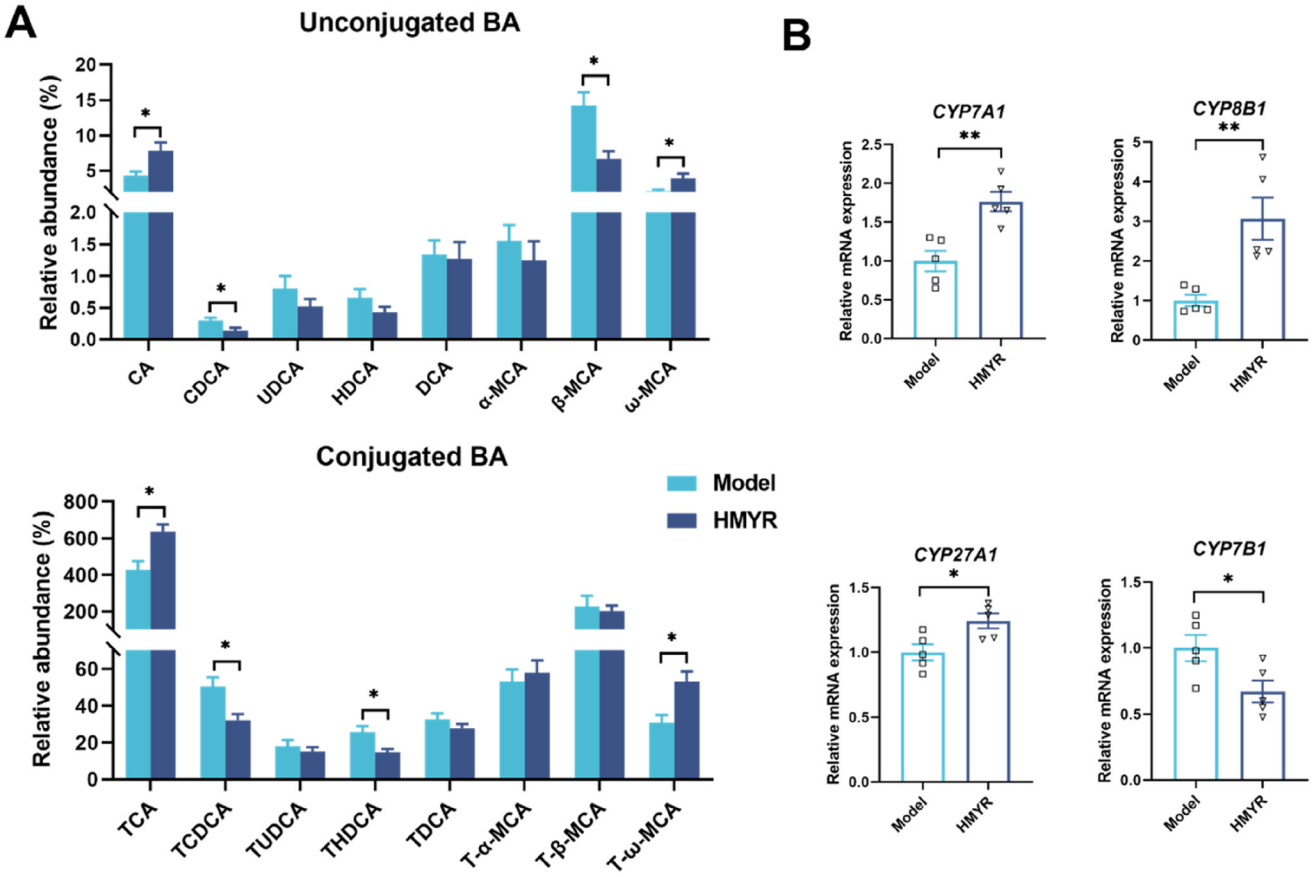

Fig. 6 Effects of MYR on the BAs profile and related gene expression in ApoE$^{-/-}$ mice. (A) The relative abundance of hepatic BAs in MYR-treated ApoE$^{-/-}$ mice (n = 7 per group). (B) Expression of key genes in hepatic BAs synthesis in MYR-treated ApoE$^{-/-}$ mice (n = 5 per group). CA, cholic acid; CDCA, chenodeoxycholic acid; UDCA, ursodeoxycholic acid; HDCA, hyodeoxycholic acid; DCA, deoxycholic acid; α-MCA, α-muricholic acid; β-MCA, β-muricholic acid; ω-MCA, ω-muricholic acid; TCA, taurocholic acid; TCDCA, tauro-chenodeoxycholic acid; TUDCA, tauro-ursodeoxycholic acid; THDCA, tauro-hyodeoxycholic acid; TDCA, tauro-deoxycholic acid; T-α-MCA, tauro-α-muricholic acid; T-β-MCA, tauro-β-muricholic acid; T-ω-MCA, tauro-ω-muricholic acid; *CYP7A1*, cholesterol 7 α-hydroxylase; *CYP8B1*, sterol 12 α-hydroxylase; *CYP27A1*, sterol 27-hydroxylase; *CYP7B1*, steroid 7-alpha-hydroxylas. Data are expressed as the mean ± SEM. * $p < 0.05$, ** $p < 0.01$, HMYR *vs.* Model.

pathways and modulation of gut microbiota community (Fig. 7). In detail, MYR upregulated *CYP7A1* and *CYP8B1* in the classical bile acids synthesis pathway, leading to an increase in hepatic CA content. The relative expression of CDCA was reduced through the downregulation of *CYP7B1*, a key enzyme in the alternative synthesis pathway of bile acids.[48] The synthesized bile acids were stored in the gall bladder, subsequently secreted into the intestine, and interacted with the gut microbiota. The relative abundance of the probiotic *g_Lachnospiraceae_NK4A136* increased, and the abundances of obesity-related genera including *g_Rikenellaceae_RC9_gut_group* and *g_Alistipes* decreased. This shift in gut microbiota composition could be attributed to the altered bile acid metabolism induced by MYR, as bile acids play a critical role in shaping the microbiota and promoting the growth of beneficial gut bacteria. For instance, *Lactobacillus* species, which were increased by MYR in our study, have been reported to regulate bile salt hydrolase activity, potentially altering bile acid pools and metabolic pathways.[51] Bile salt hydrolase from certain bacteria, including members of the *Lachnospiraceae* family, was reported to possess acyltransferase activity that enables the production of microbially conjugated bile acids through amino acid conjugation to bile acids.[52] This activity significantly diversifies the bile acid pool and can influence the gut microbiome and host health. Impact of MYR on the gut microbiota and bile acid metabolism also plays critical roles in lipid homeostasis. Previous studies have shown that MYR can alter the composition of the gut microbiota, which in turn can affect lipid absorption and metabolism.[32] The changes in bile acids observed in our study could further support this mechanism, as bile acids are involved in the emulsification and absorption of dietary lipids,[44] and alterations in bile acid signaling can influence lipid metabolism and the formation of atherogenic lipoproteins.[53] Therefore, these findings suggested that anti-atherosclerotic effects of MYR could, in part, be mediated through its influence on the gut-liver axis, which regulates lipid metabolism.

Open Access Article. Published on 06 March 2025. Downloaded on 3/20/2026 12:09:17 PM.
This article is licensed under a Creative Commons Attribution-NonCommercial 3.0 Unported Licence.

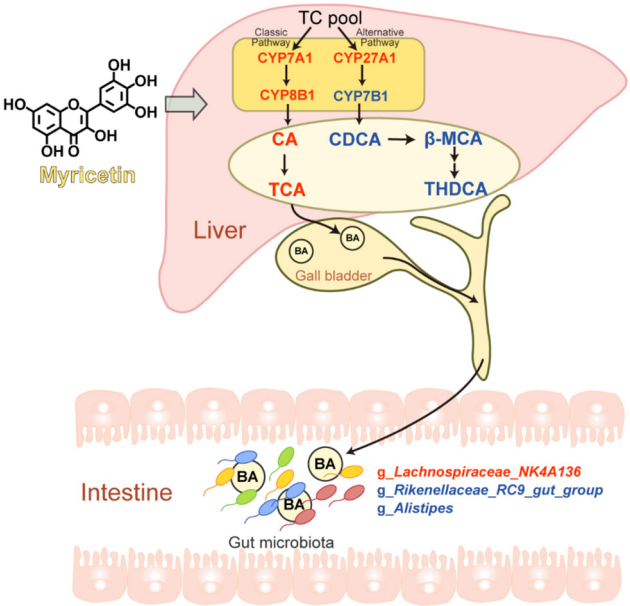

Fig. 7 Proposed mechanism of anti-atherosclerotic effect of MYR in ApoE$^{-/-}$ mice. TC, total cholesterol; BA, bile acid. Red indicates up-regulation; blue indicates down-regulation.

In recent years, an increasing body of reports has shown that the gut-liver axis plays a crucial role in preserving metabolic balance and preventing metabolic disorders such as atherosclerosis, and modifying the gut-liver axis through dietary interventions has been regarded as effective strategies for the management of metabolic diseases.[53,54] Several studies have demonstrated the significant effects of dietary flavonoids on lipid metabolism regulation and their beneficial influence on the gut-liver axis.[55] For instance, luteolin was shown to restore gut microbiota imbalance associated with the gut-liver axis and alleviate non-alcoholic fatty liver disease in HFD-fed rats.[56] Additionally, the flavonol quercetin exhibited protective effects against HFD-induced non-alcoholic fatty liver disease by modulating intestinal microbiota imbalance and activating the gut-liver axis.[57] Another studies indicated that quercetin reduced atherosclerotic lesions by altering gut microbiota composition and decreasing atherogenic lipid metabolites.[58,59] These findings collectively suggested that dietary flavonoids held great potential for the treatment of atherosclerosis through modulation of the gut-liver axis. The phenotype of MYR in reducing atherosclerosis has been reported in previous studies,[60,61] however, no further work has been carried out to explore the underlying mechanism in HFD-induced ApoE$^{-/-}$ mice. Our study contributes to this growing body of knowledge by suggesting that the beneficial effect of MYR on atherosclerosis might be associated with the regulation of the gut-liver axis. Within the gut-liver circulation, recirculated bile acids undergo partial modifications by the microbiota. However, further studies are warranted to confirm and elucidate the intricate interaction between bile acids and microbiota in the gut induced by MYR.

In this study, two different dosages of 50 and 100 mg per kg BW per day were used to investigate the potential anti-atherosclerotic effects of MYR in the ApoE$^{-/-}$ mouse model of atherosclerosis. These doses are approximately equivalent to 3.5 and 7 g day^{-1} in humans, respectively. While these doses are much higher than typical dietary flavonoid intake, which generally does not exceed 1 g of total flavonoids per day,[62] MYR constitutes only a small fraction of the total flavonoid intake. For example, the average daily intake of MYR in the adult population of South Korea is estimated to be 0.8 mg,[63] and in the adult population of the European, it is around 2 mg.[64] Therefore, while high doses of MYR were effective in the ApoE knockout mouse model, pharmacological doses may be required in humans to achieve a therapeutic effect. Additionally, the rapid progression of atherosclerosis in the ApoE knockout mouse model (within 14 weeks) contrasts with the long timeline for atherosclerosis development in humans, underscoring the differences in disease progression between animal models and human conditions. Moreover, humans and mice metabolize flavonoids differently, which could influence the bioavailability and therapeutic efficacy of MYR. Thus, future clinical studies would be required to determine the optimal dose and long-term safety of MYR for cardiovascular disease prevention and treatment in humans.

In conclusion, MYR showed a protective effect against atherosclerosis in HFD-induced ApoE$^{-/-}$ mice *via* regulating bile acids synthesis involved in gut microbiota remodeling. The anti-atherosclerosis function of MYR was associated with the increase of classical bile acids synthesis by up-regulating *CYP7A1* and *CYP8B1* expression. Such modulation, in turn, influenced the abundance of specific microbial taxa, including *g_Lachnospiraceae_NK4A136*, *g_Rikenellaceae_RC9_gut_group* and *g_Alistipes*. These findings provide valuable insights into the mechanisms by which flavonols, such as MYR, attenuate atherosclerosis. Moreover, they hold significance for the development of functional foods enriched with flavonoids as potential interventions for atherosclerosis prevention and cardiovascular health.

Data availability

The data supporting this article have been included as part of the ESI.†

Conflicts of interest

The authors declare no conflict of interest.

Acknowledgements

This work was supported by the National Natural Science Foundation of China (32372667), the Key Research and Development Program of Zhejiang Province (2021C02001), and the 111 project (B17039). We thank Zhejiang Lanxi Bayberry

Open Access Article. Published on 06 March 2025. Downloaded on 3/20/2026 12:09:17 PM.
This article is licensed under a Creative Commons Attribution-NonCommercial 3.0 Unported Licence.

Science and Technology Backyard for providing resources and assistance during the study. We also thank Zhejiang Chengfenbao Biotechnology Co., Ltd. for their technical support in metabolomics analysis.

References

1 E. Falk, Pathogenesis of atherosclerosis, *J. Am. Coll. Cardiol.*, 2006, **47**(8 Suppl), C7–C12, DOI: 10.1016/j.jacc.2005.09.068.

2 GBD 2013 Mortality and Causes of Death Collaborators, Global, regional, and national age-sex specific all-cause and cause-specific mortality for 240 causes of death, 1990–2013: a systematic analysis for the Global Burden of Disease Study 2013, *Lancet*, 2015, **385**(9963), 117–171, DOI: 10.1016/S0140-6736(14)61682-2.

3 P. Libby, The changing landscape of atherosclerosis, *Nature*, 2021, **592**(7855), 524–533, DOI: 10.1038/s41586-021-03392-8.

4 A. A. Kei, T. D. Filippatos and M. S. Elisaf, The safety of ezetimibe and simvastatin combination for the treatment of hypercholesterolemia, *Expert Opin. Drug Saf.*, 2016, **15**(4), 559–569, DOI: 10.1517/14740338.2016.1157164.

5 I. A. Mansi, E. M. Mortensen, M. J. Pugh, M. Wegner and C. R. Frei, Incidence of musculoskeletal and neoplastic diseases in patients on statin therapy: Results of a retrospective cohort analysis, *Am. J. Med. Sci.*, 2013, **345**(5), 343–348, DOI: 10.1097/MAJ.0b013e31825b8edf.

6 G. Riccardi, A. Giosuè, I. Calabrese and O. Vaccaro, Dietary recommendations for prevention of atherosclerosis, *Cardiovasc. Res.*, 2022, **118**(5), 1188–1204, DOI: 10.1093/cvr/cvab173.

7 J. A. Wali, N. Jarzebska, D. Raubenheimer, S. J. Simpson, R. N. Rodionov and J. F. O'Sullivan, Cardio-metabolic effects of high-fat diets and their underlying mechanisms-A narrative review, *Nutrients*, 2020, **12**(5), 1505, DOI: 10.3390/nu12051505.

8 W. S. Weintraub, Is atherosclerotic vascular disease related to a high-fat diet?, *J. Clin. Epidemiol.*, 2002, **55**(11), 1064–1074, DOI: 10.1016/s0895-4356(02)00541-3.

9 E. C. Aguilar, W. Fernandes-Braga, P. C. L. Leocádio, G. P. Campos, V. S. Lemos, R. P. de Oliveira, A. M. Caetano de Faria, L. Dos Santos Aggum Capettini and J. I. Alvarez-Leite, Dietary gluten worsens hepatic steatosis by increasing inflammation and oxidative stress in ApoE$^{-/-}$ mice fed a high-fat diet, *Food Funct.*, 2023, **14**(7), 3332–3347, DOI: 10.1039/d3fo00149k.

10 J. W. E. Moss, J. O. Williams, W. Al-Ahmadi, V. O'Morain, Y. H. Chan, T. R. Hughes, J. B. Menendez-Gonzalez, A. Almotiri, S. F. Plummer, N. P. Rodrigues, D. R. Michael and D. P. Ramji, Protective effects of a unique combination of nutritionally active ingredients on risk factors and gene expression associated with atherosclerosis in C57BL/6J mice fed a high fat diet, *Food Funct.*, 2021, **12**(8), 3657–3671, DOI: 10.1039/d0fo02867c.

11 T. Behl, S. Bungau, K. Kumar, G. Zengin, F. Khan, A. Kumar, R. Kaur, T. Venkatachalam, D. M. Tit, C. M. Vesa, G. Barsan and D. E. Mosteanu, Pleotropic effects of polyphenols in cardiovascular system, *Biomed. Pharmacother.*, 2020, **130**, 110714, DOI: 10.1016/j.biopha.2020.110714.

12 A. Sanches-Silva, L. Testai, S. F. Nabavi, M. Battino, K. Pandima Devi, S. Tejada, A. Sureda, S. Xu, B. Yousefi, M. Majidinia, G. L. Russo, T. Efferth, S. M. Nabavi and M. H. Farzaei, Therapeutic potential of polyphenols in cardiovascular diseases: Regulation of mTOR signaling pathway, *Pharmacol. Res.*, 2020, **152**, 104626, DOI: 10.1016/j.phrs.2019.104626.

13 X. Song, L. Tan, M. Wang, C. Ren, C. Guo, B. Yang, Y. Ren, Z. Cao, Y. Li and J. Pei, Myricetin: A review of the most recent research, *Biomed. Pharmacother.*, 2021, **134**, 111017, DOI: 10.1016/j.biopha.2020.111017.

14 R. Bertin, Z. Chen, R. Marin, M. Donati, A. Feltrinelli, M. Montopoli, S. Zambon, E. Manzato and G. Froldi, Activity of myricetin and other plant-derived polyhydroxyl compounds in human LDL and human vascular endothelial cells against oxidative stress, *Biomed. Pharmacother.*, 2016, **82**, 472–478, DOI: 10.1016/j.biopha.2016.05.019.

15 A. H. Rahmani, A. Almatroudi, K. S. Allemailem, W. M. Alwanian, B. F. Alharbi, F. Alrumaihi, A. A. Khan and S. A. Almatroodi, Myricetin: A significant emphasis on its anticancer potential via the modulation of inflammation and signal transduction pathways, *Int. J. Mol. Sci.*, 2023, **24**(11), 9665, DOI: 10.3390/ijms24119665.

16 W. H. Tang, T. Kitai and S. L. Hazen, Gut microbiota in cardiovascular health and disease, *Circ. Res.*, 2017, **120**(7), 1183–1196, DOI: 10.1161/CIRCRESAHA.117.309715.

17 M. Witkowski, T. L. Weeks and S. L. Hazen, Gut microbiota and cardiovascular disease, *Circ. Res.*, 2020, **127**(4), 553–570, DOI: 10.1161/CIRCRESAHA.120.316242.

18 A. L. Jonsson and F. Bäckhed, Role of gut microbiota in atherosclerosis, *Nat. Rev. Cardiol.*, 2017, **14**(2), 79–87, DOI: 10.1038/nrcardio.2016.183.

19 B. Guan, J. Tong, H. Hao, Z. Yang, K. Chen, H. Xu and A. Wang, Bile acid coordinates microbiota homeostasis and systemic immunometabolism in cardiometabolic diseases, *Acta Pharm. Sin. B*, 2022, **12**(5), 2129–2149, DOI: 10.1016/j.apsb.2021.12.011.

20 T. Q. de Aguiar Vallim, E. J. Tarling and P. A. Edwards, Pleiotropic roles of bile acids in metabolism, *Cell Metab.*, 2013, **17**(5), 657–669, DOI: 10.1016/j.cmet.2013.03.013.

21 A. Wang, B. Guan, C. Shao, L. Zhao, Q. Li, H. Hao, Z. Gao, K. Chen, Y. Hou and H. Xu, Qing-Xin-Jie-Yu Granule alleviates atherosclerosis by reshaping gut microbiota and metabolic homeostasis of ApoE$^{-/-}$ mice, *Phytomedicine*, 2022, **103**, 154220, DOI: 10.1016/j.phymed.2022.154220.

22 Q. Lyu, R. A. Chen, H. L. Chuang, H. B. Zou, L. Liu, L. K. Sung, P. Y. Liu, H. Y. Wu, H. Y. Chang, W. J. Cheng, W. K. Wu, M. S. Wu and C. C. Hsu, *Bifidobacterium* alleviate metabolic disorders via converting methionine to 5′-methylthioadenosine, *Gut Microbes*, 2024, **16**(1), 2300847, DOI: 10.1080/19490976.2023.2300847.

Open Access Article. Published on 06 March 2025. Downloaded on 3/20/2026 12:09:17 PM.
This article is licensed under a Creative Commons Attribution-NonCommercial 3.0 Unported Licence.

23 Y. Nakashima, A. S. Plump, E. W. Raines, J. L. Breslow and R. Ross, ApoE-deficient mice develop lesions of all phases of atherosclerosis throughout the arterial tree, *Arterioscler. Thromb.*, 1994, **14**(1), 133–140, DOI: 10.1161/01.atv.14.1.133.

24 J. Phie, S. M. Krishna, J. V. Moxon, S. M. Omer, R. Kinobe and J. Golledge, Flavonols reduce aortic atherosclerosis lesion area in apolipoprotein E deficient mice: A systematic review and meta-analysis, *PLoS One*, 2017, **12**(7), e0181832, DOI: 10.1371/journal.pone.0181832.

25 P. Libby, J. E. Buring, L. Badimon, G. K. Hansson, J. Deanfield, M. S. Bittencourt, L. Tokgözoğlu and E. F. Lewis, Atherosclerosis, *Nat. Rev. Dis. Primers*, 2019, **5**(1), 56, DOI: 10.1038/s41572-019-0106-z.

26 H. N. Ginsberg, C. J. Packard, M. J. Chapman, J. Borén, C. A. Aguilar-Salinas, M. Averna, B. A. Ference, D. Gaudet, R. A. Hegele, S. Kersten, G. F. Lewis, A. H. Lichtenstein, P. Moulin, B. G. Nordestgaard, A. T. Remaley, B. Staels, E. S. G. Stroes, M. R. Taskinen, L. S. Tokgözoğlu, A. Tybjaerg-Hansen, J. K. Stock and A. L. Catapano, Triglyceride-rich lipoproteins and their remnants: Metabolic insights, role in atherosclerotic cardiovascular disease, and emerging therapeutic strategies-a consensus statement from the European Atherosclerosis Society, *Eur. Heart J.*, 2021, **42**(47), 4791–4806, DOI: 10.1093/eurheartj/ehab551.

27 A. Ajoolabady, D. Pratico, L. Lin, C. S. Mantzoros, S. Bahijri, J. Tuomilehto and J. Ren, Inflammation in atherosclerosis: Pathophysiology and mechanisms, *Cell Death Dis.*, 2024, **15**(11), 817, DOI: 10.1038/s41419-024-07166-8.

28 G. S. Getz and C. A. Reardon, ApoE knockout and knockin mice: The history of their contribution to the understanding of atherogenesis, *J. Lipid Res.*, 2016, **57**(5), 758–766, DOI: 10.1194/jlr.R067249.

29 N. Kandasamy and N. Ashokkumar, Myricetin modulates streptozotocin-cadmium induced oxidative stress in long term experimental diabetic nephrotoxic rats, *J. Funct. Foods*, 2013, **5**(3), 1466–1477, DOI: 10.1016/j.jff.2013.06.004.

30 Z. J. Yang, H. R. Wang, Y. L. Wang, Z. H. Zhai, L. W. Wang, L. Li, C. Zhang and L. Tang, Myricetin attenuated diabetes-associated kidney injuries and dysfunction *via* regulating nuclear factor (erythroid derived 2)-like 2 and nuclear factor-κB signaling, *Front. Pharmacol.*, 2019, **10**, 647, DOI: 10.3389/fphar.2019.00647.

31 I. M. Liu, T. F. Tzeng, S. S. Liou and T. W. Lan, Myricetin, a naturally occurring flavonol, ameliorates insulin resistance induced by a high-fructose diet in rats, *Life Sci.*, 2007, **81**(21–22), 1479–1488, DOI: 10.1016/j.lfs.2007.08.045.

32 W. L. Sun, X. Y. Li, H. Y. Dou, X. D. Wang, J. D. Li, L. Shen and H. F. Ji, Myricetin supplementation decreases hepatic lipid synthesis and inflammation by modulating gut microbiota, *Cell Rep.*, 2021, **36**(9), 109641, DOI: 10.1016/j.celrep.2021.109641.

33 L. Ma, Y. Ni, Z. Wang, W. Tu, L. Ni, F. Zhuge, A. Zheng, L. Hu, Y. Zhao, L. Zheng and Z. Fu, Spermidine improves gut barrier integrity and gut microbiota function in diet-induced obese mice, *Gut Microbes*, 2020, **12**(1), 1–19, DOI: 10.1080/19490976.2020.1832857.

34 H. Li, F. Liu, J. Lu, J. Shi, J. Guan, F. Yan, B. Li and G. Huo, Probiotic mixture of *Lactobacillus plantarum* strains improves lipid metabolism and gut microbiota structure in high fat diet-fed mice, *Front. Microbiol.*, 2020, **11**(512), DOI: 10.3389/fmicb.2020.00512.

35 S. Yang, T. Hu, H. Liu, Y. L. Lv, W. Zhang, H. Li, L. Xuan, L. L. Gong and L. H. Liu, Akebia saponin D ameliorates metabolic syndrome (MetS) via remodeling gut microbiota and attenuating intestinal barrier injury, *Biomed. Pharmacother.*, 2021, **138**, 111441, DOI: 10.1016/j.biopha.2021.111441.

36 X. Kang, S. K. Ng, C. Liu, Y. Lin, Y. Zhou, T. N. Y. Kwong, Y. Ni, T. Y. T. Lam, W. K. K. Wu, H. Wei, J. J. Y. Sung, J. Yu and S. H. Wong, Altered gut microbiota of obesity subjects promotes colorectal carcinogenesis in mice, *EbioMedicine*, 2023, **93**, 104670, DOI: 10.1016/j.ebiom.2023.104670.

37 N. Ozato, T. Yamaguchi, K. Mori, M. Katashima, M. Kumagai, K. Murashita, Y. Katsuragi, Y. Tamada, M. Kakuta, S. Imoto, K. Ihara and S. Nakaji, Two *Blautia* species associated with visceral fat accumulation: A one-year longitudinal study, *Biology*, 2022, **11**(2), 318, DOI: 10.3390/biology11020318.

38 I. J. Malesza, M. Malesza, J. Walkowiak, N. Mussin, D. Walkowiak, R. Aringazina, J. Bartkowiak-Wieczorek and E. Mądry, High-fat, Western-style diet, systemic inflammation, and gut microbiota: A narrative review, *Cells*, 2021, **10**(11), 3164, DOI: 10.3390/cells10113164.

39 X. H. Yu, D. W. Zhang, X. L. Zheng and C. K. Tang, Cholesterol transport system: An integrated cholesterol transport model involved in atherosclerosis, *Prog. Lipid Res.*, 2019, **73**, 65–91, DOI: 10.1016/j.plipres.2018.12.002.

40 A. Kontush, HDL and reverse remnant-cholesterol transport (RRT): Relevance to cardiovascular disease, *Trends Mol. Med.*, 2020, **26**(12), 1086–1100, DOI: 10.1016/j.molmed.2020.07.005.

41 A. K. Groen, V. W. Bloks, H. Verkade and F. Kuipers, Cross-talk between liver and intestine in control of cholesterol and energy homeostasis, *Mol. Aspects Med.*, 2014, **37**, 77–88, DOI: 10.1016/j.mam.2014.02.001.

42 H. Li, X. H. Yu, X. Ou, X. P. Ouyang and C. K. Tang, Hepatic cholesterol transport and its role in non-alcoholic fatty liver disease and atherosclerosis, *Prog. Lipid Res.*, 2021, **83**, 101109, DOI: 10.1016/j.plipres.2021.101109.

43 K. E. Mercer, A. Maurer, L. M. Pack, K. Ono-Moore, B. J. Spray, C. Campbell, C. J. Chandler, D. Burnett, E. Souza, G. Casazza, N. Keim, J. Newman, G. Hunter, J. Fernadez, W. T. Garvey, M. E. Harper, C. Hoppel, S. H. Adams and J. Thyfault, Exercise training and diet-induced weight loss increase markers of hepatic bile acid (BA) synthesis and reduce serum total BA concentrations in obese women, *Am. J. Physiol. Endocrinol. Metab.*, 2021, **320**(5), E864–E873, DOI: 10.1152/ajpendo.00644.2020.

 This journal is © The Royal Society of Chemistry 2025

Open Access Article. Published on 06 March 2025. Downloaded on 3/20/2026 12:09:17 PM.
This article is licensed under a Creative Commons Attribution-NonCommercial 3.0 Unported Licence.

44 Y. Wang, S. Gunewardena, F. Li, D. J. Matye, C. Chen, X. Chao, T. Jung, Y. Zhang, M. Czerwiński, H. M. Ni, W. X. Ding and T. Li, An FGF15/19-TFEB regulatory loop controls hepatic cholesterol and bile acid homeostasis, *Nat. Commun.*, 2020, **11**(1), 3612, DOI: 10.1038/s41467-020-17363-6.

45 S. L. Collins, J. G. Stine, J. E. Bisanz, C. D. Okafor and A. Patterson, Bile acids and the gut microbiota: Metabolic interactions and impacts on disease, *Nat. Rev. Microbiol.*, 2023, **21**(4), 236–247, DOI: 10.1038/s41579-022-00805-x.

46 D. Rizzolo, B. Kong, R. E. Taylor, A. Brinker, M. Goedken, B. Buckley and G. L. Guo, Bile acid homeostasis in female mice deficient in *Cyp7a1* and *Cyp27a1*, *Acta Pharm. Sin. B*, 2021, **11**(12), 3847–3856, DOI: 10.1016/j.apsb.2021.05.023.

47 K. He, X. Li, Y. Xiao, Y. Yong, Z. Zhang, S. Li, T. Zhou, D. Yang, P. Gao and X. Xin, Hypolipidemic effects of *Myrica rubra* extracts and main compounds in C57BL/6j mice, *Food Funct.*, 2016, **7**(8), 3505–3515, DOI: 10.1039/c6fo00623j.

48 W. Jia, M. Wei, C. Rajani and X. Zheng, Targeting the alternative bile acid synthetic pathway for metabolic diseases, *Protein Cell*, 2021, **12**(5), 411–425, DOI: 10.1007/s13238-020-00804-9.

49 A. Wahlström, S. I. Sayin, H. U. Marschall and F. Bäckhed, Intestinal crosstalk between bile acids and microbiota and its impact on host metabolism, *Cell Metab.*, 2016, **24**(1), 41–50, DOI: 10.1016/j.cmet.2016.05.005.

50 J. M. Ridlon, D. J. Kang and P. B. Hylemon, Bile salt biotransformations by human intestinal bacteria, *J. Lipid Res.*, 2006, **47**(2), 241–259, DOI: 10.1194/jlr.R500013-JLR200.

51 Z. Song, Y. Cai, X. Lao, X. Wang, X. Lin, Y. Cui, P. K. Kalavagunta, J. Liao, L. Jin, J. Shang and J. Li, Taxonomic profiling and populational patterns of bacterial bile salt hydrolase (BSH) genes based on worldwide human gut microbiome, *Microbiome*, 2019, **7**(1), 9, DOI: 10.1186/s40168-019-0628-3.

52 D. V. Guzior, M. Okros, M. Shivel, B. Armwald, C. Bridges, Y. Fu, C. Martin, A. L. Schilmiller, W. M. Miller, K. M. Ziegler, M. D. Sims, M. E. Maddens, S. F. Graham, R. P. Hausinger and R. A. Quinn, Bile salt hydrolase acyltransferase activity expands bile acid diversity, *Nature*, 2024, **626**(8000), 852–858, DOI: 10.1038/s41586-024-07017-8.

53 R. Duan, X. Guan, K. Huang, Y. Zhang, S. Li, J. Xia and M. Shen, Flavonoids from whole-grain oat alleviated high-fat diet-induced hyperlipidemia via regulating bile acid metabolism and gut microbiota in mice, *J. Agric. Food Chem.*, 2021, **69**(27), 7629–7640, DOI: 10.1021/acs.jafc.1c01813.

54 Q. Hu, W. Zhang, Z. Wu, X. Tian, J. Xiang, L. Li, Z. Li, X. Peng, S. Wei, X. Ma and Y. Zhao, Baicalin and the liver-gut system: Pharmacological bases explaining its therapeutic effects, *Pharmacol. Res.*, 2021, **165**, 105444, DOI: 10.1016/j.phrs.2021.105444.

55 L. Zhao, S. Wang, N. Zhang, J. Zhou, A. Mehmood, R. N. Raka, F. Zhou and L. Zhao, The beneficial effects of natural extracts and bioactive compounds on the gut-liver axis: A promising intervention for alcoholic liver disease, *Antioxidants*, 2022, **11**(6), 1211, DOI: 10.3390/antiox11061211.

56 X. Liu, R. Sun, Z. Li, R. Xiao, P. Lv, X. Sun, M. A. Olson and Y. Gong, Luteolin alleviates non-alcoholic fatty liver disease in rats via restoration of intestinal mucosal barrier damage and microbiota imbalance involving in gut-liver axis, *Arch. Biochem. Biophys.*, 2021, **711**, 109019, DOI: 10.1016/j.abb.2021.109019.

57 D. Porras, E. Nistal, S. Martínez-Flórez, S. Pisonero-Vaquero, J. L. Olcoz, R. Jover, J. González-Gallego, M. V. García-Mediavilla and S. Sánchez-Campos, Protective effect of quercetin on high-fat diet-induced non-alcoholic fatty liver disease in mice is mediated by modulating intestinal microbiota imbalance and related gut-liver axis activation, *Free Radicals Biol. Med.*, 2017, **102**, 188–202, DOI: 10.1016/j.freeradbiomed.2016.11.037.

58 J. Nie, L. Zhang, G. Zhao and X. Du, Quercetin reduces atherosclerotic lesions by altering the gut microbiota and reducing atherogenic lipid metabolites, *J. Appl. Microbiol.*, 2019, **127**(6), 1824–1834, DOI: 10.1111/jam.14441.

59 K. Kasahara, R. L. Kerby, R. Aquino-Martinez, A. H. Evered, T. L. Cross, J. Everhart, T. K. Ulland, C. D. Kay, B. W. Bolling, F. Bäckhed and F. E. Rey, Gut microbes modulate the effects of the flavonoid quercetin on atherosclerosis, *npj Biofilms Microbiomes*, 2025, **11**(1), 12, DOI: 10.1038/s41522-024-00626-1.

60 Y. Sasaki, K. Hyodo, A. Hoshino, E. Kisa, K. Matsuda, Y. Horikawa and J. Giddings, Myricetin and hesperidin inhibit cerebral thrombogenesis and atherogenesis in Apoe$^{-/-}$ and Ldlr$^{-/-}$ mice, *Food Nutr. Sci.*, 2018, **9**, 20–31, DOI: 10.4236/fns.2018.91002.

61 Z. Meng, M. Wang, J. Xing, Y. Liu and H. Li, Myricetin ameliorates atherosclerosis in the low-density-lipoprotein receptor knockout mice by suppression of cholesterol accumulation in macrophage foam cells, *Nutr. Metab.*, 2019, **16**, 25, DOI: 10.1186/s12986-019-0354-7.

62 P. Mullie, P. Clarys, P. Deriemaeker and M. Hebbelinck, Estimation of daily human intake of food flavonoids, *Plant Foods Hum. Nutr.*, 2007, **62**, 93–98, DOI: 10.1007/s11130-007-0047-7.

63 S. Jun, S. Shin and H. Joung, Estimation of dietary flavonoid intake and major food sources of Korean adults, *Br. J. Nutr.*, 2016, **115**(3), 480–489, DOI: 10.1017/S0007114515004006.

64 A. Vogiatzoglou, A. A. Mulligan, M. A. H. Lentjes, R. N. Luben, J. P. E. Spencer, H. Schroeter, K. T. Khaw and G. G. C. Kuhnle, Flavonoid intake in European adults (18 to 64 years), *PLoS One*, 2015, **10**(5), e0128132, DOI: 10.1371/journal.pone.0128132.